LIMNOLOGY and OCEANOGRAPHY LETTERS

ASLO

Open Access

Limnology and Oceanography Letters 11, 2026, e70098

doi: 10.1002/lol2.70098

LETTER

Tropical river discharge dominates riverine carbon export to Australia's coastal waters

Francesco Ulloa-Cedamanos [1]* Adam T. Rexroade [1] Anna Lintern [2] Marcus B. Wallin [3] Yihan Li [1,4] Dylan J. Irvine [1,5] Lindsay B. Hutley [1] Josep G. Canadell [6] Judith A. Rosentreter [7] Jacob Z.-Q. Yeo [7] Bradley D. Eyre [7] David E. Butman [8] Clément Duvert [1,5,9]*

[1]Faculty of Science and Technology, Research Institute for the Environment and Livelihoods, Charles Darwin University, Darwin, Northwest Territories, Australia; [2]Department of Civil Engineering, Monash University, Clayton, Victoria, Australia; [3]Department of Aquatic Sciences and Assessment, Swedish University of Agricultural Sciences, Uppsala, Sweden; [4]School of Hydraulic Engineering, Zhejiang University of Water Resources and Electric Power, Hangzhou, China; [5]National Centre for Groundwater Research and Training, Bedford Park, South Australia, Australia; [6]CSIRO Environment, Canberra, Australian Capital Territory, Australia; [7]Faculty of Science and Engineering, Southern Cross University, Lismore, New South Wales, Australia; [8]School of Environmental and Forest Sciences, University of Washington, Seattle, Washington, USA; [9]College of Science and Engineering, James Cook University, Cairns, Queensland, Australia

Scientific Significance Statement

Rivers are critical conduits for transporting carbon (C) from terrestrial ecosystems to coastal waters, yet limited data have hindered robust national-scale estimates of riverine C export. In Australia, a continent of contrasting climate zones, the spatial and seasonal patterns of riverine C fluxes have remained poorly understood. By integrating an extensive national C database with modeled discharge, this study provides the 1st continent-wide assessment of Australia's riverine C export, revealing that tropical rivers—despite covering less than a 3rd of the continent—dominate Australia's riverine C export due to their high and seasonally pulsed discharge.

Abstract

Rivers play a crucial role in the transformation and export of carbon (C) to coastal waters, yet limited observations in Australia have hindered accurate C flux estimates. We compiled 27,696 dissolved inorganic C (DIC), 15,012 dissolved organic C (DOC), and 226 particulate organic C (POC) measurements in Australian rivers and combined these with modeled discharge to estimate Australian-scale C export. Annual riverine C export was 19.1 (6.1–47.9) $\times$ 10^3 Gg C yr^{-1}, with DIC and DOC exports 2.9 and 2.7 times higher than previous estimates, while POC was 2.6 times lower. The Australian tropics contributed 65%, 39%, and 66% of national DIC, DOC, and POC exports, respectively, despite covering only 11% of exorheic Australia. Within tropical basins, wet-season C export was 158–423 times higher than dry-season C export. These findings underscore the dominant influence of tropical rivers and their strong seasonal pulse on Australia's riverine C export.

*Correspondence: francesco.ulloacedamanos@cdu.edu.au; clem.duvert@cdu.edu.au

Associate editor: Susana Bernal

Rivers and streams are key components of the global carbon (C) cycle, acting as conduits for export of terrestrial C to coastal ecosystems along the land-to-ocean aquatic continuum (LOAC) (Regnier et al. 2022). The annual transfer of C from terrestrial landscapes to riverine networks is estimated at 2–3 $\times 10^6$ Gg C yr^{-1} (Regnier et al. 2022; Battin et al. 2023). Once in fluvial systems, this C can be exchanged with the atmosphere, buried in sediments, or transported downstream to estuaries and coastal waters (Cole et al. 2007; Bauer et al. 2013; P. A. Raymond et al. 2013). Given these roles, improving estimates of land-to-ocean C fluxes across spatial scales is critical to inform C budgeting efforts (Canadell et al. 2011, 2023).

Recent estimates place global LOAC export in the range of 0.8–1.3 $\times 10^6$ Gg C yr^{-1} (Regnier et al. 2022; Canadell et al. 2023). Compared to other LOAC components, such as land-to-river C inputs or river-to-atmosphere C emissions, riverine C export to the ocean is easier to quantify from observations. Nonetheless, while numerous global estimates of riverine C export have been produced over the past decades (e.g., Li et al. 2017; Ludwig and Probst 1996; Regnier et al. 2022), recent studies reveal substantial variability among estimates, particularly when different C species (i.e., inorganic and organic C) are considered separately. These differences are even more pronounced at regional or continental scales. Notably, Oceania—particularly Australia—exhibits some of the highest discrepancies in model-derived estimates across C species, reflecting data scarcity in this region (M. Liu et al. 2024). A recent modeling effort that provided a continent-wide C budget for Australia included a preliminary estimate of riverine C export to the ocean at $8.7 \pm 4.4 \times 10^3$ Gg C yr^{-1} (Villalobos et al. 2023). However, estimates from that study remain uncertain, as DOC observations relied on global datasets rather than Australia-specific data (Harrison et al. 2005), and DIC observations were limited to southeastern Australia (Hartmann et al. 2014). This limited data coverage may not have captured the unique hydroclimatic and landscape characteristics of Australian rivers (Shanafield et al. 2024).

Estimating riverine C export to the ocean relies on either empirical or process-based models, both of which are constrained by the availability, representativeness, and quality of C data (Müller et al. 2022). Process-based models such as ORCHIDEE-$C_{lateral}$, which has been used in Europe (H. Zhang et al. 2022), carry large uncertainties due to the limited understanding of key drivers of C transport and transformation along the LOAC (Lauerwald et al. 2020). Discrepancies between models are typically more pronounced at the catchment scale, where fine-scale variability is challenging to capture (M. Liu et al. 2024). Although field surveys offer the most accurate means of estimating riverine C export on a regional scale, their application is limited by logistical and financial constraints (Li et al. 2017). To address data gaps, statistical approaches such as random forest models have been increasingly applied to estimate riverine C export to the ocean, including in China (Yan et al. 2023) and globally (M. Liu et al. 2024). However, these approaches remain limited by data coverage and the resolution and quality of predictor variables. Given these limitations, region-specific assessments grounded in direct observations remain essential for improving our understanding of C export dynamics.

In this context, we aim to establish the most comprehensive data-derived estimates of riverine C export to estuaries and coastal waters across Australia by integrating new and existing C observations with model-based river discharge estimates. We assessed the export patterns and rates of dissolved inorganic C (DIC), dissolved organic C (DOC), and particulate organic C (POC) at a monthly time step to integrate temporal variability in C export. Our approach involved assessing data reliability, addressing spatial gaps, and quantifying uncertainty based on model fit, which was propagated to flux estimates using a bootstrapping approach.

Methods

A brief description of main land uses and climatic characteristics across Australia, along with corresponding maps (Supporting Information Fig. S1), is provided in the Extended Methods section of the Supporting Information.

Data sources

Our analysis follows the Bureau of Meteorology's classification of Australia into 13 major hydrological basins (called drainage divisions), which are further subdivided into 219 river regions. When excluding endorheic basins, 12 drainage divisions and 188 river regions discharge into coastal waters (Supporting Information Fig. S2A), with over 95% of them covering areas greater than 700 km^2 (Supporting Information Fig. S2B). Modeled daily runoff data (mm d^{-1}) were sourced for each river region from the Australian Landscape Water Balance model (Frost and Shokri 2021). We also considered six broad climate classes based on the Köppen–Geiger classification (Beck et al. 2018), with each river region outlet and each sampled site assigned a climate class (Supporting Information Fig. S1). Lastly, the extent of carbonate lithology was identified for each river region from the Surface Geology of Australia dataset (O. Raymond et al. 2012).

The C concentration data (in mg L^{-1}) comprise measured and estimated DIC, as well as DOC and POC records spanning the period between 1966 to 2024 across all 12 exorheic drainage divisions (Fig. 1; Supporting Information Table S1). We used the OzRiCa database (Ulloa-Cedamanos et al. 2025), which we expanded with an additional 182 DIC, 189 DOC, and 149 POC observations from more recent peer-reviewed literature and previously unpublished data (Supporting Information Table S2). The expanded dataset comprised 36,691 DIC (mean $\pm \sigma = 14.1 \pm 15.7$ mg L^{-1}), 19,116 DOC (8.8 ± 11.8 mg L^{-1}), and 226 POC (1.1 ± 2.0 mg L^{-1}) observations. Particulate inorganic carbon (PIC) was not included in

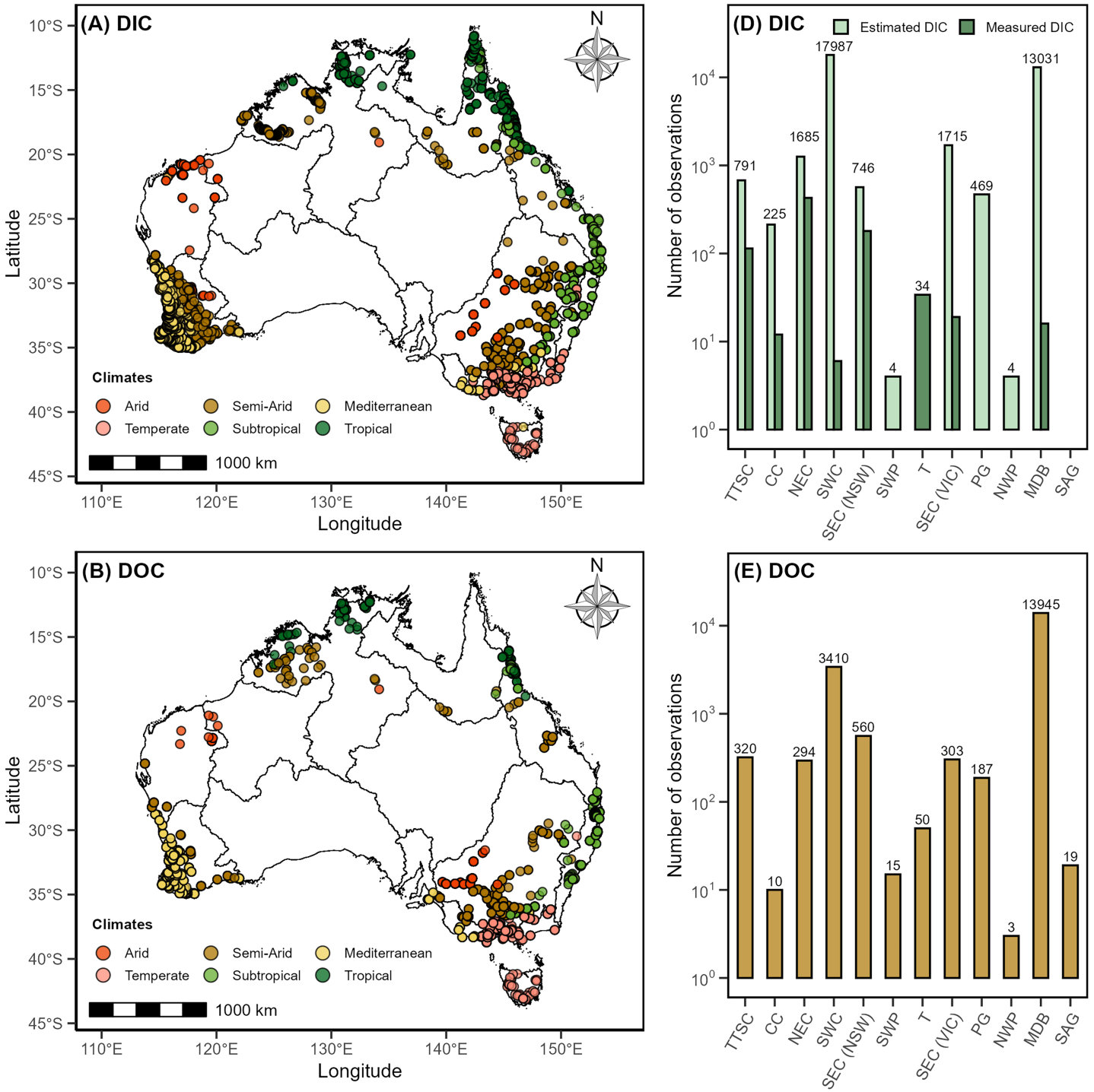

Fig. 1. Spatial distribution (**A–C**) and number of observations of riverine carbon concentrations compiled in the selected riverine C dataset (**D–F**). Rows show DIC (**A**, **D**), DOC (**B**, **E**), and POC (**C**, **F**). Markers are colored according to climate classes. Data are split into 12 exorheic drainage divisions based on classification from the Bureau of Meteorology. The drainage divisions are: Tanami–Timor Sea Coast (TTSC), Carpentaria Coast (CC), Northeast Coast (NEC), Southwest Coast (SWC), Southeast Coast–New South Wales (SEC-NSW), Southwestern Plateau (SWP), Tasmania (T), Southeast Coast–Victoria (SEC-VIC), Pilbara–Gascoyne (PG), Northwestern Plateau (NWP), Murray–Darling Basin (MDB), and South Australian Gulf (SAG).

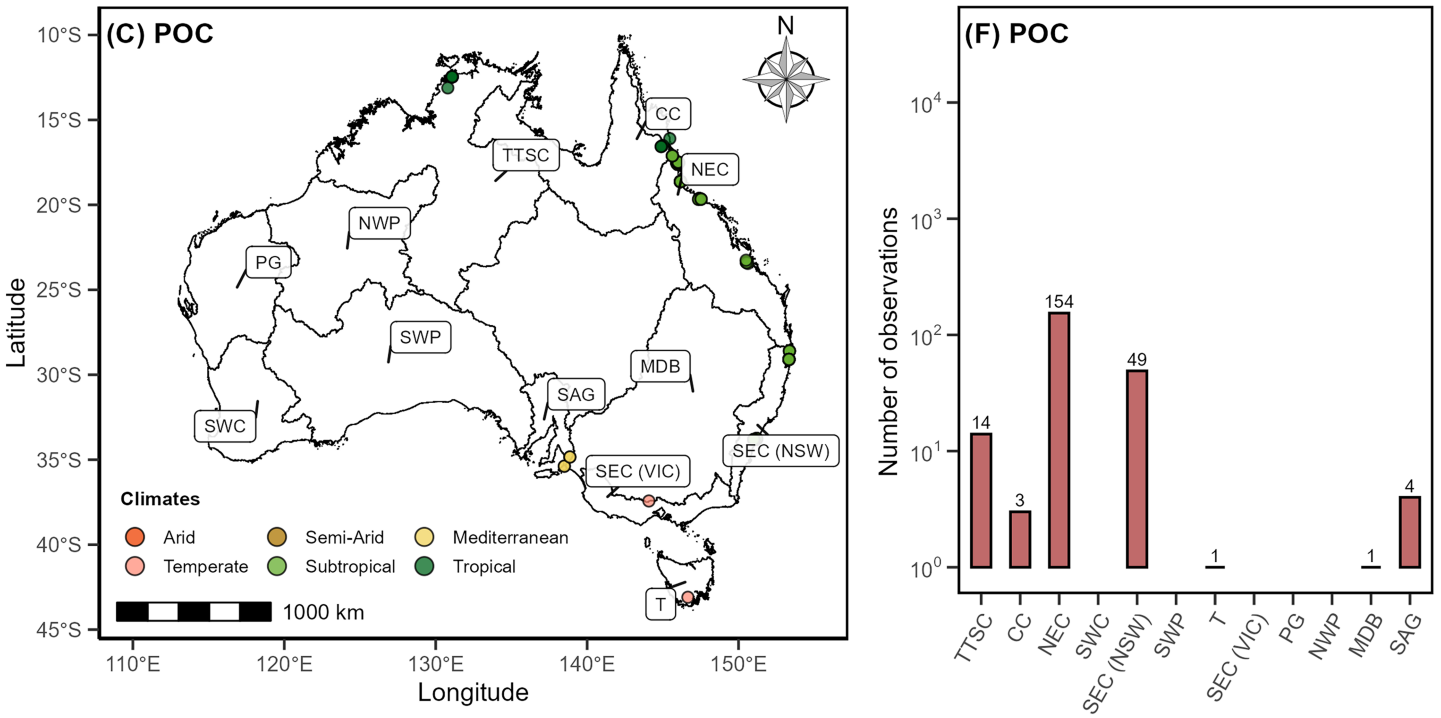

Fig. 1. Continued

this study due to the lack of available data at the national scale and its likely negligible contribution to C fluxes due to progressive trapping before reaching the coast (Probst et al. 1994). Estimated DIC concentrations were calculated from alkalinity, pH, and temperature; validation of this approach using sites with both measured and estimated DIC showed high agreement ($R^2 > 0.99$, $p < 0.01$, Supporting Information Fig. S3).

Data processing

We derived long-term, ensemble monthly mean discharge ($Q_{i,r}$) and DIC, DOC, and POC concentrations ($C_{i,r}$) for each river region (r) and calendar month (i) over the period 2014–2023. This process allowed us to define a "typical" hydrological year, facilitating analyses based on seasons, rather than on year-to-year variability. The 2014–2023 period was selected to ensure that Q values reflect contemporary hydrological conditions. Comparisons with the full 1950–2023 Australian Landscape Water Balance model database confirmed the representativeness of this subset of Q data (Supporting Information Fig. S4).

We assessed the reliability of Australian Landscape Water Balance model derived Q estimates using quality-checked times-series of measured Q from 25 Hydrologic Reference Stations (X. S. Zhang et al. 2016) across Australia (Supporting Information Fig. S1D). Australian Landscape Water Balance model tended to underestimate flows overall by 19%, with larger underestimation in arid regions (up to 79%) but minimal bias in tropical and subtropical regions. Despite this, ensemble monthly mean Q showed a significant correlation with observations ($p < 0.01$; Supporting Information Fig. S5). To address this bias and account for the skewed distribution of Q, we applied a bootstrapping approach (1000 iterations with replacement, using the R *boot* package) to generate ensemble monthly mean Q estimates ($Q_{i,r}$) and their uncertainty bounds ($Q_{i,r\_\min}$ and $Q_{i,r\_\max}$ based on the P5 and P95 percentiles). This method avoids assumptions about the distribution of Q and captures its variability, thereby reducing bias in estimated C fluxes.

Data on C concentration were not available for all drainage divisions (Fig. 1), river regions, stream orders (Supporting Information Fig. S6) or months (Supporting Information Fig. S7). Across the 188 river regions, monthly concentration data were available for 36% and 19% of all DIC and DOC region–month combinations, respectively. Missing data were gap-filled using interannual means from the same month and river region (47% and 65% gaps filled for DIC and DOC, respectively), same drainage division (11% and 16% gaps filled for DIC and DOC, respectively), or the whole of Australia (6% gaps filled for DIC). Spatial gaps (Fig. 1) limited coastal representation, with only half of the sites located within 25 km of the coastal line. To overcome this, DOC and DIC data from low stream orders (1–4) were used to approximate concentrations in high-order rivers (5–9) only when concentrations for

a given drainage division were not statistically different between low- and high-order rivers (Wilcoxon signed-rank test, Supporting Information Table S3), which occurred in 10 out of the 18 drainage divisions. Dissolved inorganic C and DOC data in low-order streams from the remaining drainage divisions were excluded, reducing the initial database to 42,934 observations (Supporting Information Table S1). Ensemble monthly (i) mean C concentrations ($C_{i,r}$) were then calculated for each river region (r), along with the P5 ($C_{i,r\_\min}$) and P95 ($C_{i,r\_\max}$) percentiles. Due to scarcity of POC observations (Fig. 1), we applied a more conservative statistical approach calculating the ensemble monthly mean of POC concentrations (C_i) with the P5 ($C_{i\_\min}$) and P95 ($C_{i\_\max}$) percentiles across all available data rather than by river region. Applying the same approach used for POC to DIC and DOC resulted in minimal differences at the national scale, but led to either overestimation or underestimation (> 60%) at the drainage division scale. Further evaluation of our Q, DIC, DOC, and POC estimates, and a sensitivity analysis comparing the use of mean vs. median values for flux estimation are provided in the Extended Methods (Supporting Information).

Carbon export and uncertainty estimate

Ensemble monthly mean C export ($F_{i,r}$, in Gg yr^{-1}, Eq. 1) was calculated by multiplying ensemble mean C concentrations ($C_{i,r}$ for DIC and DOC or C_i for POC) by ensemble mean Q ($Q_{i,r}$) for each month (i) and river region (r). Uncertainty ranges were defined by P5 ($F_{i,r\_\min}$) and P95 ($F_{i,r\_\max}$).

$$F_{i,r} = C_{i,r}\,(\text{or}\,C_i) \times Q_{i,r} \quad (1)$$

Ensemble annual C export ($F_{\text{annual},r}$, in Gg yr^{-1}, Eq. 2) and associated uncertainties were calculated by summing up the ensemble monthly C exports ($F_{i,r}$) for each river region (r):

$$F_{\text{annual},r} = \sum F_{i,r} \quad (2)$$

We also estimated the export of C species for each of our six broad climate classes by first calculating the share of total runoff contributed by each climate class within each drainage division (Supporting Information Table S4). We then allocated C exports in proportion to these runoff contributions, and summed up the values of each climate class across all drainage divisions.

Results

Carbon concentrations and spatial coverage

Dissolved inorganic C concentrations were higher in sites where DIC was measured than in sites where DIC was estimated ($p = 0.01$; Wilcoxon rank-sum test), with extreme values being more common in the latter. Mean, median, and interquartile range were highest for DIC, followed by DOC and POC, while variability showed an inverse pattern, with POC exhibiting the highest coefficient of variation (Supporting Information Table S1).

Dissolved inorganic C had the highest number of measured and estimated observations ($n = 27{,}696$), with most DIC data from the Southwest Coast (46% of total DIC observations) and Murray–Darling Basin (41%) regions. Similarly to DIC, most DOC observations ($n = 15{,}012$) were recorded in the Murray–Darling Basin (87%) and Southwest Coast (7%). In contrast, most POC data ($n = 42$) were collected in Northeast Coast (67%) and Southeast Coast–New South Wales (NSW) (21%) (Fig. 1). Records of DIC and DOC were particularly scarce in the Northwestern Plateau, South Australian Gulf, and Southwestern Plateau. These drainage divisions are characterized by low runoff (< 30 mm y r^{-1}, Table 1), and a lower prevalence of permanent streams and rivers (Shanafield et al. 2024). Particulate organic C records were limited overall, with only Northeast Coast, Southeast Coast–NSW, and Tasmania with more than 10 observations (Fig. 1).

Seasonal changes in riverine C export

Mean monthly riverine C export exhibited pronounced seasonal variability across Australia's drainage divisions (Fig. 2). Dissolved inorganic C exports ranged from 22 (1.7–94) $\times 10^{-9}$ Gg month^{-1} in July to 956 (436–1701) Gg month^{-1} in February, both observed in Carpentaria Coast. Dissolved organic C exports ranged from 13 (0.2–30) $\times 10^{-9}$ Gg month^{-1} in July in the Tanami–Timor Sea Coast division to 251 (25–744) Gg month^{-1} in July in Southwest Coast, while POC exports ranged from 1.8 (0.0003–8.7) $\times 10^{-9}$ Gg month^{-1} in August to 98 (1.7–417) Gg month^{-1} in February, with both extremes occurring in Tanami–Timor Sea Coast.

Riverine C exports closely followed the seasonal Q patterns (Table 1; Supporting Information Fig. S4), with variability within and across drainage divisions reflecting differences in regional climates (Fig. 2; Supporting Information Fig. S1; Table 2). In tropical regions, C exports peaked during the wet season (November to April) and were markedly higher than during the dry season (May to October), ranging from 158-fold higher for DIC in Tanami–Timor Sea Coast to 423-fold higher for POC in Carpentaria Coast. A similar but less intense pattern was observed in subtropical Northeast Coast and Southeast Coast–NSW. In contrast, temperate and Mediterranean regions like Southeast Coast–Victoria, Tasmania and Southwest Coast exhibited peak exports during cooler months (June to September), consistent with the winter-dominated rainfall regime in southern rivers. Meanwhile, arid and semi-arid regions showed more heterogeneous patterns, with lower C export yields in the northwest compared to southern Australia despite similarly low runoff.

Spatial patterns in riverine C export

Our national mean riverine C export estimates amounted to 12.3 (4.1–31.4) $\times 10^3$ Gg C yr^{-1} for DIC (65% of total export), 5.8 (1.9–13.2) $\times 10^3$ Gg C yr^{-1} for DOC (31% of total export) and 0.9 (0.1–3.3) $\times 10^3$ Gg C yr^{-1} for POC (5%

Table 1. Summary of exorheic drainage division characteristics, including surface area (km^2), carbonate outcrop coverage (%), ensemble mean flow (*Q*, in TL yr^{-1} and mm yr^{-1}), dominant climate type, and carbon exports (flux: Gg C yr^{-1}; yield: kg C km^{-2} yr^{-1}) for DIC, DOC, and POC. Flux values represent medians, with 5th and 95th percentiles shown in brackets. The 12 drainage divisions are: Tanami–Timor Sea Coast (TTSC), Carpentaria Coast (CC), Northeast Coast (NEC), Southwest Coast (SWC), Southeast Coast–New South Wales (SEC-NSW), Southwestern Plateau (SWP), Tasmania (T), Southeast Coast–Victoria (SEC-VIC), Pilbara–Gascoyne (PG), Northwestern Plateau (NWP), Murray–Darling Basin (MDB), and South Australian Gulf (SAG). Dominant climates were assigned based on the major contributors (>50%) to total annual runoff in each drainage division (Supporting Information Table S4). If no single climate exceeded 50%, the 1st two largest contributing climates were reported.

	Surface area	Carbonate outcrops	*Q*		Dominant climates	DIC				DOC				POC			
						Flux	5th	95th	Yield	Flux	5th	95th	Yield	Flux	5th	95th	Yield
Drainage division	km^2	%	TL yr^{-1}	Mm yr^{-1}		Gg C yr^{-1}			kg C km^{-2} yr^{-1}	Gg C yr^{-1}			kg C km^{-2} yr^{-1}	Gg C yr^{-1}			kg C km^{-2} yr^{-1}
TTSC	1,156,708	3.9	310	268	Tropical	2715	795	6049	2347	1471.2	495	3214	1271.9	374.2	28	1288	323.5
CC	639,740	9.5	172	269	Tropical	5352	1930	14,925	8366	791.8	317	1420	1237.7	223.8	13	813	349.8
NEC	451,608	0.2	113	251	Tropical and subtropical	1326	191	4187	2937	854.5	251	1937	1892.1	127.7	8	505	282.8
SWC	325,904	0.2	62	191	Mediterranean	664	342	1155	2036	1320.1	290	3563	4050.7	58.1	11	211	178.3
SEC-NSW	129,333	2.1	39	299	Subtropical	715	139	1937	5530	243.8	40	768	1885.1	41	2	190	317
SWP	1,094,045	17.1	31	29	Arid	1073	565	1761	981	641.1	302	1135	585.9	24.2	4.2	97	22.2
T	68,251	4.6	27	402	Temperate	244	140	399	3569	260.5	125	473	3817.1	26.2	4.2	94	383.7
SEC-VIC	135,036	5.1	13	18	Temperate	87	24	244	646	165.8	70	361	1228.1	4.4	0.6	17	32.7
PG	477,893	9.0	5.5	41	Arid	87	5.4	466	183	35.4	3.8	131	74	3.9	0.2	21	8.2
NWP	719,996	1.0	3.7	7.8	Arid	60	3.5	190	83	40.2	2.8	108	55.8	17.4	0.2	106	24.1
MDB	1,062,118	2.8	0.8	0.8	Temperate and semi-arid	10	0.2	59	9.6	5.1	0.2	31.7	4.8	0.6	0.0	3.8	0.6
SAG	116,865	2.5	0.3	2.9	Mediterranean	5.5	1.4	15	47	5.9	2.3	11	50.4	0.3	0.0	1.5	2.9
Exorheic Australia*	6,377,497	6.1	777.3	121.9		12,339	4135	31,386	2228	5835	1899	13,153	1346	902	71	3346	160

*Exorheic Australia excludes the endorheic Lake Eyre Basin since this drainage division does not discharge into the ocean.

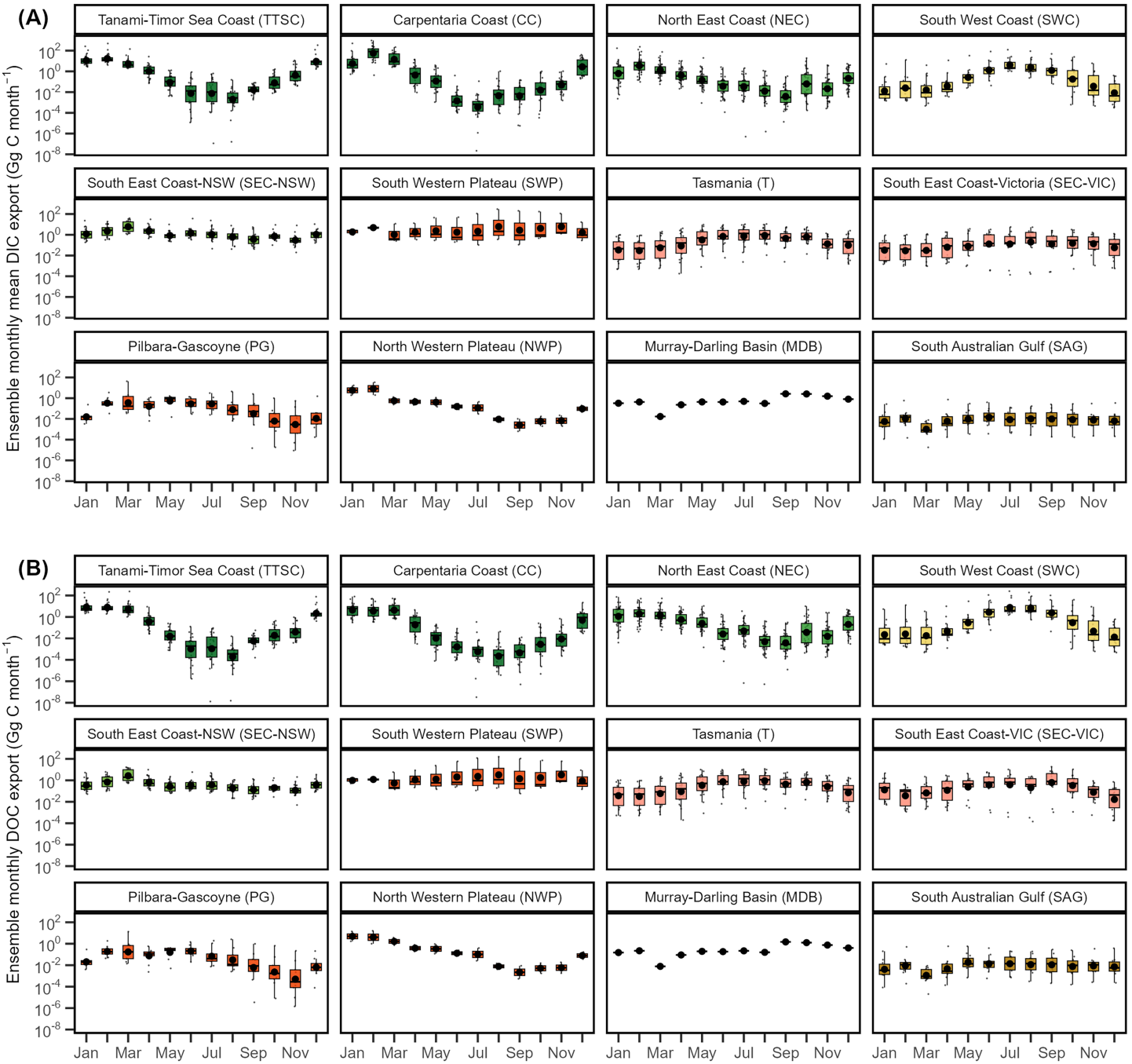

Fig. 2. Ensemble monthly mean (**A**) DIC, (**B**) DOC, and (**C**) POC exports (in Gg C month^{-1}), grouped by exorheic drainage division. Box plots reflect variability among contributing river regions within each division. Colors indicate the dominant climate within each drainage division. The y-axis is log-scaled, and black dots show monthly means. Drainage divisions are ordered by decreasing total discharge (Table 1).

of total export), for a total C export of 19.1 (6.1–47.9) × 10^3 Gg C yr^{-1}. The ensemble mean riverine C exports varied substantially across drainage divisions and C species. DIC, DOC, and POC export ranged from 5.5, 5.1, and 0.3 Gg yr^{-1} in South Australian Gulf, Murray–Darling Basin, and South Australian Gulf to as high as 5352, 1471, and 374 Gg yr^{-1} in Carpentaria Coast, Tanami–Timor Sea Coast and Tanami–Timor Sea Coast, respectively (Table 1). These variations were primarily driven by differences in *Q*, with higher *Q* in rivers of the tropical North (Carpentaria Coast and Tanami–Timor Sea Coast in Supporting Information Fig. S4) leading to higher C export—although some variations were also linked to

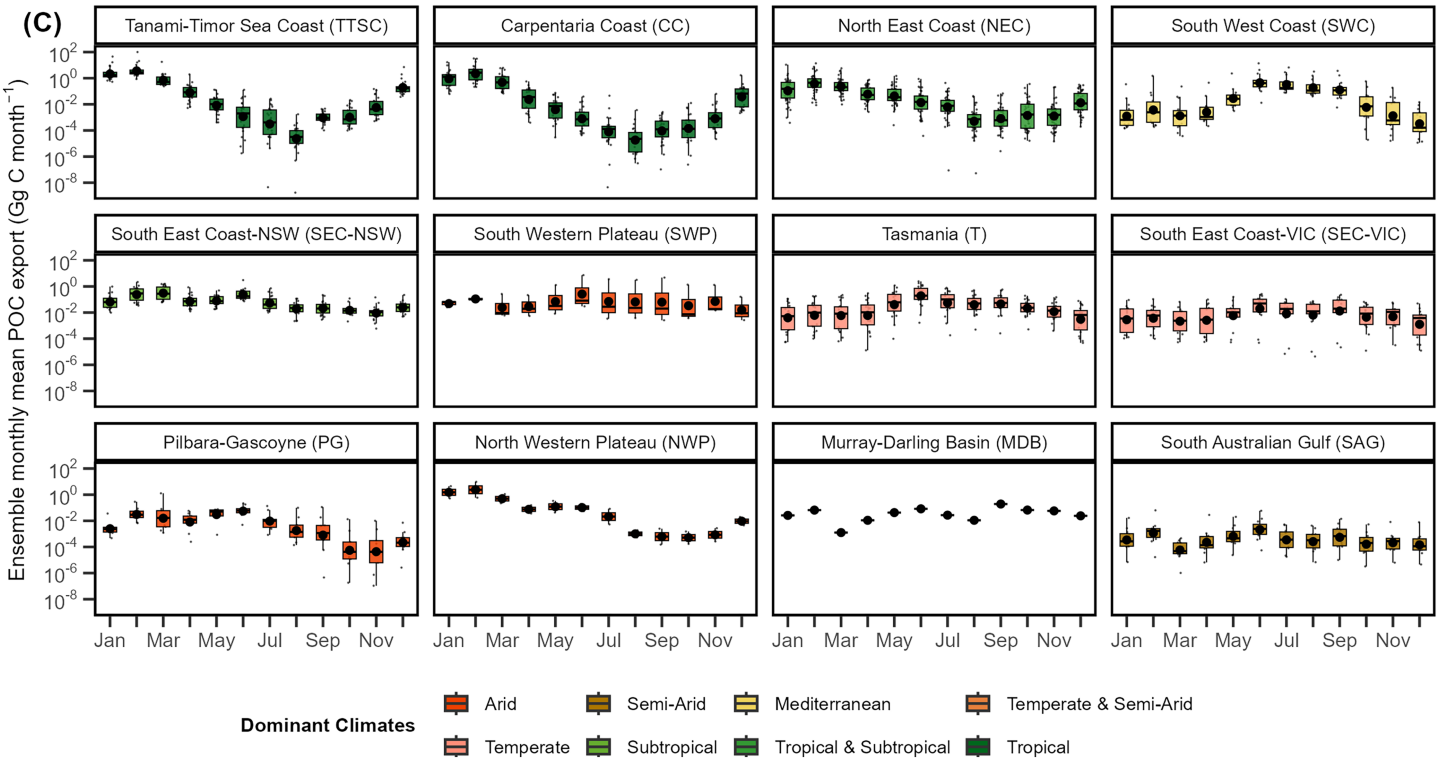

Fig. 2. Continued

Table 2. Partitioning of DIC, DOC, and POC export across six broad climate regions in Australia.

Parameter	Units	Tropical	Subtropical	Mediterranean	Temperate	Semi-arid	Arid	Total
Surface area	km^2	685,418	360,715	208,076	292,447	1,885,638	2,935,635	6,367,929
	%	10.8	5.7	3.3	4.6	29.6	46.1	100
DIC	Gg C yr^{-1}	6339	1020	750	633	2382	1215	12,340
DOC		1943	486	1322	514	856	715	5836
POC		466	77	58	48	190	62	902
Total C export	Gg C yr^{-1}	8748	1584	2130	1195	3429	1993	19,078
	%	45.9	8.3	11.2	6.3	18.0	10.4	100

differences in C concentrations, particularly for DOC where concentrations were also higher in the Southwest Coast. Drainage divisions such as Pilbara–Gascoyne, Northwestern Plateau, Murray–Darling Basin, and South Australian Gulf consistently showed low exports of DIC, DOC, and POC, reflecting their limited runoff and arid to semi-arid conditions.

When normalized by drainage area, ensemble mean C yields generally mirrored regional runoff patterns. Tasmania displayed the highest yields, in line with high annual runoff. Outliers in wetter regions included Carpentaria Coast for DIC and Southwest Coast for DOC, both of which showed higher yields than drainage divisions with similar or greater runoff. In drier regions with annual runoff below 100 mm yr^{-1}, Southwestern Plateau for DIC and Southeast Coast–Victoria for DOC stood out, with higher yields driven by elevated C concentrations despite limited runoff (Fig. 3). The two drainage divisions with the highest DIC yields, Carpentaria Coast and Southwestern Plateau, located in wetter and drier regions, respectively, also had the highest carbonate outcrop coverage (Table 1).

Discussion

Tropical rivers dominate C export in Australia

We found that riverine C exports are strongly influenced by hydrological patterns across Australia, with Q emerging as

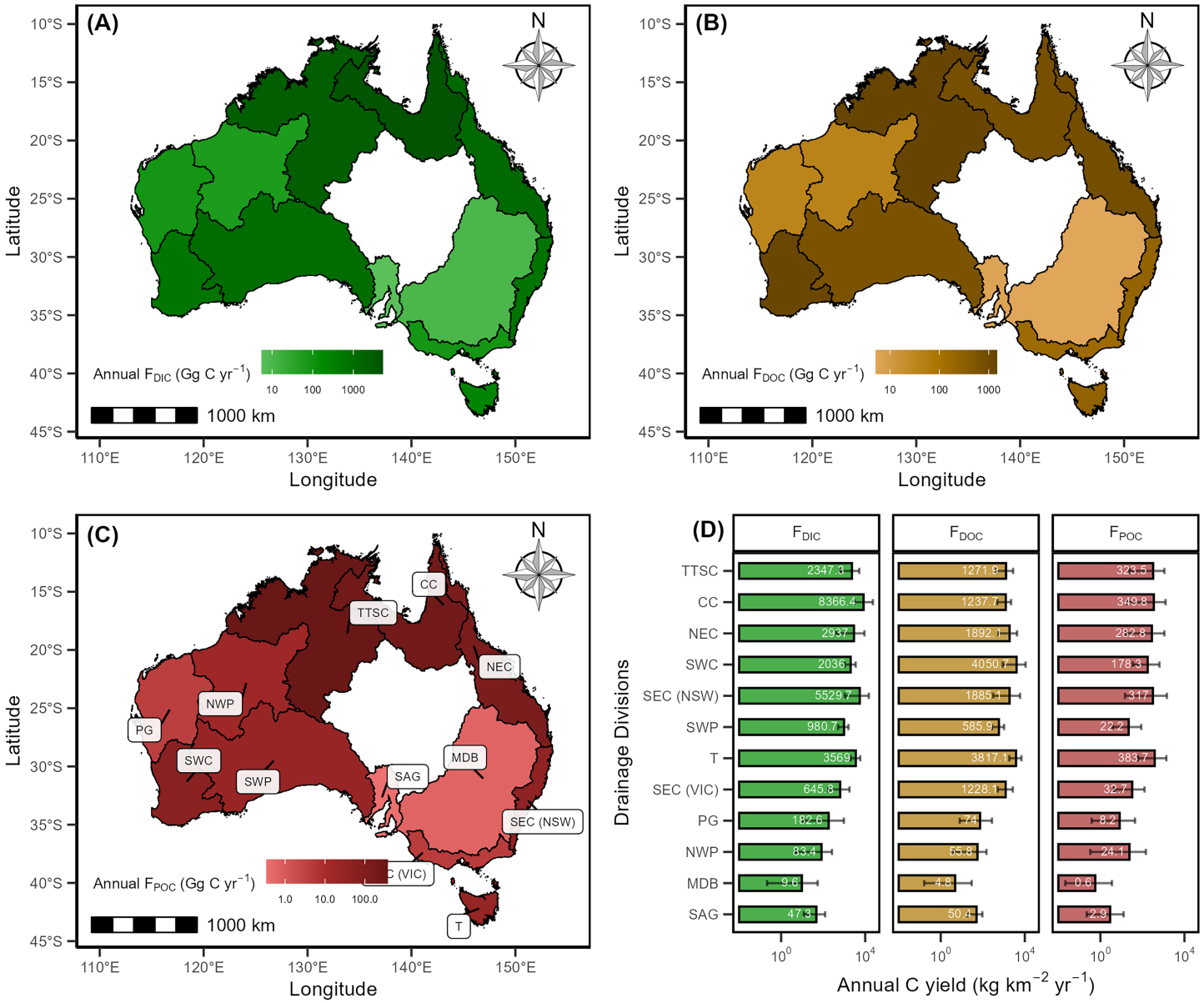

Fig. 3. Ensemble mean riverine exports (Gg C yr^{-1}) of (**A**) DIC, (**B**) DOC, and (**C**) POC across Australian drainage divisions. (**D**) Ensemble mean yields (kg C km^{-2} yr^{-1}) of DIC, DOC, and POC per drainage division, with error bars representing the 5th and 95th percentiles.

the primary driver of both dissolved and particulate C transport. This aligns with previous studies identifying surface runoff as a dominant control on C export from catchment to continental scales (e.g., Zhong et al. 2017; Ulloa-Cedamanos et al. 2021a; S. Liu et al. 2022). Temporal shifts in Q closely mirrored changes in C exports across all drainage divisions (Fig. 2; Supporting Information Fig. S4A), emphasizing the tight coupling between hydrology and C mobilization. Most importantly, tropical northern regions dominated C export, with the seasonal monsoonal pulse from January to March accounting for half of the continent-wide riverine C export. In these regions, monsoonal rainfall promoted high hydrological connectivity and large pulses of C export, with exports then declining by up to two orders of magnitude during the dry season (May to October). Conversely, in the Mediterranean and temperate southern regions, rainfall mostly occurs during the Austral winter (Dey et al. 2019). We found that these winter-dominated exports of southern regions generated total C exports four times lower than the summer-dominated exports of northern regions—with the exception of the Southwest Coast, which exported large amounts of DOC due to high concentrations in that area. Annually, tropical regions

accounted for 46% of the total riverine C export, despite covering only 11% of Australia's landmass (Table 2).

Beyond hydrology, Australia's environmental heterogeneity adds further complexity to spatial C export patterns. Along the tropical northern coastline, the Tanami–Timor Sea Coast and Carpentaria Coast experience similar monsoonal rainfall and runoff regimes (Table 1), yet riverine DIC yields largely differed between them (Table 2). These differences likely reflect regional differences in land cover (Supporting Information Fig. S1) and extent of carbonate outcrops (Table 1), both of which modulate DIC production and transport (Zeng et al. 2019; S. Liu et al. 2022; Meybeck 2003; Ulloa-Cedamanos et al. 2021b; Tan et al. 2024). Consistent with this, carbonate-rich drainage divisions such as Carpentaria Coast (10% of surface area covered by carbonate outcrops) and Southwestern Plateau (17%) (Table 1) exhibited higher mean DIC concentrations (38.3 ± 68.4 mg L^{-1} for the Carpentaria Coast and 49.7 ± 38.4 mg L^{-1} for the Southwestern Plateau) than the continental mean ($p < 0.01$, Wilcoxon rank-sum test). While Q governs much of the seasonal and interannual variability, lithology likely modulated the baseline concentrations of DIC and contributed to spatial differences in C fluxes across drainage divisions.

Implications for national and global C budgets

Our new riverine C export estimate of 19.1 (6.1–47.9) $\times$ 10^3 Gg C yr^{-1} updates previous values upward, with DOC and DIC exports 2.7 and 2.9 times higher, respectively, than the corresponding estimates reported in Villalobos et al. (2023). This discrepancy largely reflects the limited Australian data used in that previous study. A more recent analysis using additional estuarine data (Reithmaier et al. 2024) also estimated lower national-scale DIC and DOC exports (10.9×10^3 Gg C yr^{-1}). Importantly, our estimates are subject to uncertainties associated with flow modeling and gaps in C observations, particularly for POC. We chose to use means rather than median Q and concentrations, as we believe they better capture the disproportionate contribution of extreme events, which are critical drivers of riverine C dynamics in Australia (Leigh et al. 2015; Moran et al. 2013). Further discussion of uncertainties is provided in the Extended Discussion (Supporting Information).

Compared with studies reporting all three C fractions from in situ measurements, our results show similar patterns but different magnitudes. High DIC fractions have been reported in carbonate-rich basins such as the Mississippi (76%, Cai et al. 2015), Yangtze (81%, L. Zhang et al. 2014), and Usumacinta rivers (85%, Soria-Reinoso et al. 2022), while our estimate (65%) is closer to silicate-dominated systems like the Yukon River (64%, Guo et al. 2012). Our DOC contribution (31%) matches global estimates (Meybeck 1993), while our POC contribution (5%) is mostly lower than previous studies. These contrasts illustrate how hydroclimate and lithology control the export of DIC, DOC, and POC.

At the global scale, Australia covers 5% of the Earth's land surface but contributes less than 2% of global riverine C exports (M. Liu et al. 2024). The C yields of Australia's tropical regions (12.8 Mg C km^{-2} yr^{-1}, Table 2) are broadly comparable to those of other tropical regions such as Southeast Asia (38.1 Mg C km^{-2} yr^{-1}) and South America (11.0 Mg C km^{-2} yr^{-1}). However, Australia's overall C yields are much lower (3.0 Mg C km^{-2} yr^{-1}) because of the relatively small extent of tropical regions (11% of exorheic Australia) compared to the more dominant arid (46%; 0.7 Mg C km^{-2} yr^{-1}) and semi-arid regions (30%; 1.8 Mg C km^{-2} yr^{-1}) (Supporting Information Fig. S1). This highlights the disproportionate role of tropical regions as hotspots of riverine C export in Australia.

This work focused on riverine C exports to estuaries and coastal waters but did not capture transport and transformation in coastal systems. At the Australian scale, estuaries and coastal wetlands—the mixing zone between the riverine and marine environments along the LOAC (Rosentreter and Eyre 2025)—transform, retain (6.5×10^3 Gg C yr^{-1}), and emit (7.3×10^3 Gg C yr^{-1}) 72.3% of the riverine C they receive, while also sequestering additional C (16.7×10^3 Gg C yr^{-1}), with the remaining portion exported to the ocean. Integrating these pathways with our estimates will provide a more complete picture of the Australian LOAC (Villalobos et al. 2023).

Author Contributions

Francesco Ulloa-Cedamanos: writing – original draft, conceptualization, methodology, data collection, software development, data curation, formal validation analysis, visualization, writing – review and editing. Adam T. Rexroade: data collection, writing – review and editing. Anna Lintern: conceptualization, methodology, writing – review and editing. Marcus B. Wallin: conceptualization, writing – review and editing. Yihan Li: data collection, writing – review and editing. Dylan J. Irvine: methodology, software development, writing – review and editing. Lindsay B. Hutley: data collection, writing – review and editing. Josep G. Canadell: writing – review and editing. Judith A. Rosentreter: data collection, writing – review and editing. Jacob Z.-Q. Yeo: data collection, writing – review and editing. Bradley D. Eyre: data collection, writing – review and editing. David E. Butman: writing – review and editing. Clément Duvert: writing – original draft, conceptualization, methodology, data collection, writing – review and editing, funding acquisition, supervision, resources.

Acknowledgments

This research was supported by the Australian Research Council (DP220100823, DE220100852).

Conflicts of Interest

The authors declare no conflicts of interest.

Data Availability Statement

Data and metadata are available in the HydroShare data repository (http://www.hydroshare.org/resource/9aa735254e7e424ca18603c047d02f50).

References

Battin, T. J., R. Lauerwald, E. S. Bernhardt, et al. 2023. "River Ecosystem Metabolism and Carbon Biogeochemistry in a Changing World." *Nature* 613: 449–459. https://doi.org/10.1038/s41586-022-05500-8.

Bauer, J. E., W.-J. Cai, P. A. Raymond, T. S. Bianchi, C. S. Hopkinson, and P. A. G. Regnier. 2013. "The Changing Carbon Cycle of the Coastal Ocean." *Nature* 504: 61–70. https://doi.org/10.1038/nature12857.

Beck, H. E., N. E. Zimmermann, T. R. McVicar, N. Vergopolan, A. Berg, and E. F. Wood. 2018. "Present and Future Köppen-Geiger Climate Classification Maps at 1-km Resolution." *Sci Data* 5: 180214. https://doi.org/10.1038/sdata.2018.214.

Cai, Y., L. Guo, X. Wang, and G. Aiken. 2015. "Abundance, Stable Isotopic Composition, and Export Fluxes of DOC, POC, and DIC From the Lower Mississippi River during 2006–2008." *Journal of Geophysical Research: Biogeosciences* 120: 2273–2288. https://doi.org/10.1002/2015JG003139.

Canadell, J. G., P. Ciais, K. Gurney, et al. 2011. "An International Effort to Quantify Regional Carbon Fluxes." *Eos, Transactions American Geophysical Union* 92: 81–82. https://doi.org/10.1029/2011EO100001.

Canadell, J. G., P. M. S. Monteiro, M. H. Coasta, et al. 2023. "Global Carbon and Other Biogeochemical Cycles and Feedbacks." In *Climate Change 2021: The Physical Science Basis. Contribution of Working Group I to the Sixth Assessment Report of the Intergovernmental Panel on Climate Change*, edited by V. Masson-Delmotte, P. Zhai, A. Pirani, et al., 673–816. Cambridge University Press.

Cole, J. J., Y. T. Prairie, N. F. Caraco, et al. 2007. "Plumbing the Global Carbon Cycle: Integrating Inland Waters into the Terrestrial Carbon Budget." *Ecosystems* 10: 171–184. https://doi.org/10.1007/s10021-006-9013-8.

Dey, R., S. C. Lewis, J. M. Arblaster, and N. J. Abram. 2019. "A Review of Past and Projected Changes in Australia's Rainfall." *WIREs Climate Change* 10: e577. https://doi.org/10.1002/wcc.577.

Frost, A. J., and A. Shokri. 2021. *The Australian Landscape Water Balance Model (AWRA-L v7)*. Bureau of Meteorology Technical Report. Technical Description of the Australian Water Resources Assessment Landscape Model Version 7.

Guo, L., Y. Cai, C. Belzile, and R. W. Macdonald. 2012. "Sources and Export Fluxes of Inorganic and Organic Carbon and Nutrient Species From the Seasonally Ice-Covered Yukon River." *Biogeochemistry* 107: 187–206. https://doi.org/10.1007/s10533-010-9545-z.

Harrison, J. A., N. Caraco, and S. P. Seitzinger. 2005. "Global Patterns and Sources of Dissolved Organic Matter Export to the Coastal Zone: Results From a Spatially Explicit, Global Model." *Global Biogeochem Cycles* 19: 1–16. https://doi.org/10.1029/2005GB002480.

Hartmann, J., R. Lauerwald, and N. Moosdorf. 2014. "A Brief Overview of the GLObal RIver Chemistry Database, GLORICH." *Procedia Earth and Planetary Science* 10: 23–27. https://doi.org/10.1016/j.proeps.2014.08.005.

Lauerwald, R., P. Regnier, B. Guenet, P. Friedlingstein, and P. Ciais. 2020. "How Simulations of the Land Carbon Sink Are Biased by Ignoring Fluvial Carbon Transfers: A Case Study for the Amazon Basin." *One Earth* 3: 226–236. https://doi.org/10.1016/j.oneear.2020.07.009.

Leigh, C., A. Bush, E. T. Harrison, et al. 2015. "Ecological Effects of Extreme Climatic Events on Riverine Ecosystems: Insights From Australia." *Freshwater Biology* 60: 2620–2638. https://doi.org/10.1111/fwb.12515.

Li, M., C. Peng, M. Wang, et al. 2017. "The Carbon Flux of Global Rivers: A Re-Evaluation of Amount and Spatial Patterns." *Ecological Indicators* 80: 40–51. https://doi.org/10.1016/j.ecolind.2017.04.049.

Liu, M., P. A. Raymond, R. Lauerwald, et al. 2024. "Global Riverine Land-to-Ocean Carbon Export Constrained by Observations and Multi-Model Assessment." *Nature Geoscience* 17: 896–904. https://doi.org/10.1038/s41561-024-01524-z.

Liu, S., C. Kuhn, G. Amatulli, et al. 2022. "The Importance of Hydrology in Routing Terrestrial Carbon to the Atmosphere Via Global Streams and Rivers." *Proceedings of the National Academy of Sciences of the United States of America* 119: 1–9. https://doi.org/10.1073/pnas.2106322119.

Ludwig, W., and J. L. Probst. 1996. "Predicting the Oceanic Input of Organic Carbon by Continental Erosion." *Global Biogeochemical Cycles* 10: 23–41. https://doi.org/10.1029/95GB02925.

Meybeck, M. 1993. "Riverine Transport of Atmospheric Carbon: Sources, Global Typology and Budget." *Water, Air, and Soil Pollution* 70: 443–463. https://doi.org/10.1007/BF01105015.

Meybeck, M. 2003. "5.08 – Global Occurrence of Major Elements in Rivers." In *Treatise on Geochemistry*, edited by H. D. Holland and K. K. Turekian, 207–224. Pergamon.

Moran, N. P., G. G. Ganf, T. A. Wallace, and J. D. Brookes. 2013. "Flow Variability and Longitudinal Characteristics of Organic Carbon in the Lachlan River, Australia." *Marine and Freshwater Research* 65: 50–58. https://doi.org/10.1071/MF12297.

Müller, G., J. Börker, A. Sluijs, and J. J. Middelburg. 2022. "Detrital Carbonate Minerals in Earth's Element Cycles." *Global Biogeochem Cycles* 36: e2021GB007231. https://doi.org/10.1029/2021GB007231.

Probst, J.-L., J. Mortatti, and Y. Tardy. 1994. "Carbon River Fluxes and Weathering CO_2 Consumption in the Congo and Amazon River Basins." *Applied Geochemistry* 9: 1–13. https://doi.org/10.1016/0883-2927(94)90047-7.

Raymond, O., S. Liu, R. Gallagher, W. Zhang, and L. Highet. 2012. *Surface Geology of Australia, 1:1 Million Scale Dataset,*

2012 Edition. Commonwealth of Australia (Geoscience Australia).

Raymond, P. A., J. Hartmann, R. Lauerwald, et al. 2013. "Global Carbon Dioxide Emissions from Inland Waters." *Nature* 503: 355–359. https://doi.org/10.1038/nature12760.

Regnier, P., L. Resplandy, R. G. Najjar, and P. Ciais. 2022. "The Land-to-Ocean Loops of the Global Carbon Cycle." *Nature* 603: 401–410. https://doi.org/10.1038/s41586-021-04339-9.

Reithmaier, G. M. S., D. T. Maher, C. Holloway, R. E. Correa, and I. R. Santos. 2024. "Small Wetland-Fringed Estuaries Deliver Disproportionately Large Carbon Loads to the Ocean." *Limnology and Oceanography* 69: 2229–2242. https://doi.org/10.1002/lno.12660.

Rosentreter, J. A., and B. D. Eyre. 2025. "Uncertainties about the Role of River and Mangrove Dissolved Inorganic Carbon and Alkalinity Loads in Buffering the Great Barrier Reef Lagoon." *Global Biogeochemical Cycles* 39: e2024GB008134. https://doi.org/10.1029/2024GB008134.

Shanafield, M., M. Blanchette, E. Daly, et al. 2024. "Australian Non-Perennial Rivers: Global Lessons and Research Opportunities." *Journal of Hydrology* 634: 130939. https://doi.org/10.1016/j.jhydrol.2024.130939.

Soria-Reinoso, I., J. Alcocer, S. Sánchez-Carrillo, et al. 2022. "The Seasonal Dynamics of Organic and Inorganic Carbon along the Tropical Usumacinta River Basin (Mexico)." *Water* 14: 1–30. https://doi.org/10.3390/w14172703.

Tan, X., H. Jiang, and Q. Zhang. 2024. "Lithology Constrains the Origination of Autochthonous Carbon in River Ecosystems." *Water Research* 260: 121860. https://doi.org/10.1016/j.watres.2024.121860.

Ulloa-Cedamanos, F., A. Probst, V. Dos-Santos, T. Camboulive, F. Granouillac, and J.-L. Probst. 2021*a*. "Stream Hydrochemical Response to Flood Events in a Multi-Lithological Karstic Catchment from the Pyrenees Mountains (SW France)." *Water* 13: 1818. https://doi.org/10.3390/w13131818.

Ulloa-Cedamanos, F., A. Probst, I. Moussa, and J.-L. Probst. 2021*b*. "Chemical Weathering and CO_2 Consumption in a Multi-Lithological Karstic Critical Zone: Long Term Hydrochemical Trends and Isotopic Survey." *Chemical Geology* 585: 120567. https://doi.org/10.1016/j.chemgeo.2021.120567.

Ulloa-Cedamanos, F., A. T. Rexroade, Y. Li, et al. 2025. "OzRiCa: An Australian Riverine Carbon Database of Concentrations, Gas Fluxes and Isotopes." *Earth System Science Data Discussions* 2025: 1–31. https://doi.org/10.5194/essd-2025-233.

Villalobos, Y., J. G. Canadell, E. D. Keller, et al. 2023. "A Comprehensive Assessment of Anthropogenic and Natural Sources and Sinks of Australasia's Carbon Budget." *Global Biogeochemical Cycles* 37: 1–25. https://doi.org/10.1029/2023GB007845.

Yan, Y., R. Lauerwald, X. Wang, et al. 2023. "Increasing Riverine Export of Dissolved Organic Carbon from China." *Global Change Biology* 29: 5014–5032. https://doi.org/10.1111/gcb.16819.

Zeng, S., Z. Liu, and G. Kaufmann. 2019. "Sensitivity of the Global Carbonate Weathering Carbon-Sink Flux to Climate and Land-Use Changes." *Nature Communications* 10: 5749. https://doi.org/10.1038/s41467-019-13772-4.

Zhang, H., R. Lauerwald, P. Ciais, K. Van Oost, B. Guenet, and P. Regnier. 2022. "Global Changes Alter the Amount and Composition of Land Carbon Deliveries to European Rivers and Seas." *Communications Earth & Environment* 3: 245. https://doi.org/10.1038/s43247-022-00575-7.

Zhang, L., M. Xue, M. Wang, W.-J. Cai, L. Wang, and Z. Yu. 2014. "The Spatiotemporal Distribution of Dissolved Inorganic and Organic Carbon in the Main Stem of the Changjiang (Yangtze) River and the Effect of the Three Gorges Reservoir." *Journal of Geophysical Research: Biogeosciences* 119: 741–757. https://doi.org/10.1002/2012JG002230.

Zhang, X. S., G. E. Amirthanathan, M. A. Bari, et al. 2016. "How Streamflow Has Changed across Australia since the 1950s: Evidence from the Network of Hydrologic Reference Stations." *Hydrology and Earth System Sciences* 20: 3947–3965. https://doi.org/10.5194/hess-20-3947-2016.

Zhong, J., S. L. Li, F. Tao, F. Yue, and C. Q. Liu. 2017. "Sensitivity of Chemical Weathering and Dissolved Carbon Dynamics to Hydrological Conditions in a Typical Karst River." *Scientific Reports* 7: 1–9. https://doi.org/10.1038/srep42944.

Supporting Information

Additional Supporting Information may be found in the online version of this article.

Submitted 06 August 2025
Revised 18 December 2025
Accepted 21 December 2025